

# Visualization of Conflict Networks

Ulrik BRANDES <sup>a</sup>, Jürgen LERNER <sup>a</sup>

<sup>a</sup> University of Konstanz

**Abstract.** Visualization is a powerful tool to derive insights from massive, noisy, and possibly inconsistent datasets. We propose a method for the visualization of conflict networks that show a set of actors together with hostile or conflictive relations on the systemic level. Our method highlights the most involved actors, reveals the opposing groups, provides a graphic overview of the conflict structure, and allows for smooth animation of the dynamics of a conflict. The visualization technique can deal with potentially complex network structures and distinguishes visually between bilateral and multilateral conflicts.

**Keywords.** Conflict data, network visualization, time-dependent visualization.

## Introduction

Event data describes “who did (when/where) what to whom” and are among the most widely used indicators in quantitative international relations research [1]. From a high level view, event data are used for two types of purposes: first, the assessment of current or past political situations, second; for statistical validation of theories about the likelihood and outcome of conflict and cooperation. Currently there exist many event databases (some of which are described in this book) that differ largely in scope, granularity, and in whether they are hand-coded or automatically extracted from, e.g., news sources. Due to the typical size of these datasets, it is hard to derive insights from them without automatic support.

In this chapter we present a method to *visualize* event data given as a set of pairwise *conflictive* or *hostile* interactions. Well-designed images of conflict data provide support for at least three different purposes. First, they give the analyst a graphic overview of the data, which may reveal expected or surprising patterns, and thereby can lead to hypotheses that may be validated or rejected later. Second, visualizing data is a powerful tool for error detection and data cleaning. Last but not least, images are very convenient to present and communicate insights to others.

A straightforward way to visualize conflicts is to make use of geographic maps and, e.g., highlight countries involved in conflicts. While such drawings have the advantage that they are very common and most people are familiar with them, a different visualization strategy can give additional insights into the data. As a matter of fact, conflicts among large sets of political actors do not normally happen at random but often reveal a grouping of actors into two or more blocks, characterized as follows: conflicts within a block are rare or weak and conflicts between actors from different blocks frequent and more serious. Groups need not be defined by official treaties or alliances but are rather determined by the interactions themselves. Naturally, this grouping of actors does not

necessarily coincide with geographic closeness or distance so that geographically determined positions do not reveal the group membership of actors. A distinguishing feature of our method is that we show the conflict *network* where actors' positions are determined by the relations themselves, thereby revealing the network's *structure*.

Given a list of events, our method visualizes the resulting conflict network in such a way that actors are far from each other if there is a strong negative (i.e., conflictive) relationship between them and close to each other if they share the same opponent(s). An example of visualization of a conflict network is shown in Fig. 1. If events have timestamps attached to them, the static visualization can be turned into an animated scatterplot showing the dynamics of major conflicts over time. From such a video, an analyst can recognize or discover the major actors engaged in conflict during certain periods of time, see how they are grouped together, and which are their main opponents. The observer is also enabled to detect time-points where the conflict structure changes significantly. Since our animation is smooth by design, it can be recognized easily which actors enter or leave a conflict during transitions. In contrast to a pure dyadic analysis, networks give additional information about indirect ties (e.g. enemies of enemies), density, complexity, and structure of the actors' network environment.

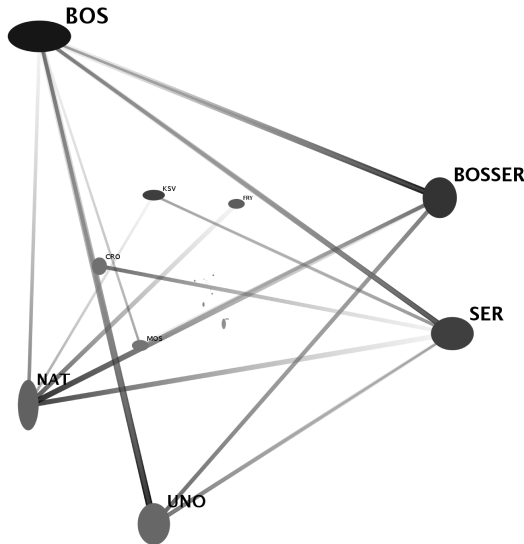


**Figure 1.** Visualization of the conflict network constructed from events related to the War in Bosnia. The nodes represent political actors, the edges represent conflictive relations which are often military engagements. Three groups that are in conflict with each other are revealed. The dominant members of these groups are {BOSSER (Serbs in Bosnia), SER (Serbia)}, {UNO, NAT (NATO)}, and {BOS (Bosnia)}.

### Related Work

Many event databases exist that differ largely in scope (e.g., which actors or events are included; which time-period is being considered) and granularity (e.g., aggregation of actors ranging from countries over ethnic groups and organizations to individual persons;

granularity of time-stamps ranging from years to days). Hand-coded datasets (such as [2, 3]) are typically coarser-grained than machine-coded event sets (such as [4,5]). King and Lowe [4] report similar performance for an automated extraction tool as for human coders. Nevertheless, it can be expected that machine-coded data is more likely to contain events that are obviously incorrect for a human coder (cf. Sect. 4.2 below). Although our method is applicable to human-coded as well as to machine-coded event data, it is especially appropriate for the visualization of large, fine-grained, and potentially noisy datasets. For the examples in this paper we use automatically coded data from the KEDS (Kansas Event Data System ) project [5].

One typical use of event data is to analyze the outcome and likelihood of conflict. For instance, Schneider and Troeger [6] examine the influence that conflicts and cooperative events in war regions have on financial markets. They demonstrate that this impact not only depends on the severity of conflicts but also on the degree to which economic agents could anticipate events. Guidolin and La Ferrara [7] analyze the effects that the onset of violent conflict has on asset markets. Schneider [8] reversed this line of research by examining how political events can be foreseen by using data from financial markets. Obviously, studies as in the three last-mentioned papers rely on the validity of conflict data, i. e., to what extent does the dataset represent the true level of conflict or cooperation at a given point in time. Thus, a possible usage scenario of our visualization technique is to detect coding errors and clean the data before doing the analysis.

While studies of conflict often focus on the dyadic level (i. e., the relationship between only two actors), there is increasing interest in applying network analysis techniques to understand world politics at the systemic level. Maoz *et al.* [9] provide an overview of the potential use of network analysis in international relations research. In many studies, network structures such as alliance and ethnic (e. g., linguistic or religious) affinity networks, as well as trade relations, are considered as independent variables from which it is sought to predict the level of conflict (cf., e. g., [10,11]). Harary [12] and Maoz *et al.* [13] analyze the *balance* (i. e., does it hold that two enemies never have common friends; is the enemy of an enemy a friend) of the network of friendship and enmity in world politics. Other papers aim to understand the effect of several structural characteristics, including reciprocity, triangularity, polarity and bipolarity, on conflict [14,15,16]. Note that the bipolarity index that we introduce in Sect. 2.1 is different from those considered by Esteban and Ray [14] since our index is defined as a function of the structure of conflictive relations. A paper closely related to ours is Häggerli *et al.* [17], who applied network analysis and visualization techniques to conflictive and cooperative relationships. The main difference is that in their paper actors that are strongly in conflict are drawn closely together, whereas our visualization technique separates strong enemies (cf. Fig. 1), thereby revealing opposing groups.

The method presented in our paper is also a tool to dynamically visualize *news* sources—a topic that has received considerable attention (cf. e. g., [18,19,20]). Wong *et al.* [21] proposed a method to generate animated scatterplots from data streams, such as sequences of news articles. (Scatterplots are widely used in statistical graphics, see, e. g., [22,23].) However, the scatterplots in [21] show similarities between documents and not hostile relationships between political actors as will be done here.

The basic version of our visualization method [24], which is restricted to display a single bipolar conflict is augmented in the current paper to deal with several and potentially multipolar conflicts.

*Outline of this paper.* In Sect. 1 we provide background information on the type of data that is being analyzed. Our method for visualizing the conflict structure embodied in a set of events is introduced in Sect. 2 and extended to smooth animation of event series in Sect. 3. The utility of our method is illustrated on event data from the Balkans in Sect. 4. We conclude with a discussion of open problems and future work.

## 1. Event Data

Our method is applicable to event data given as a series of pairwise interactions. Although it is independent of the data format, we will focus on a particular coding scheme to make the exposition more concrete. The Kansas Event Data System (KEDS) [5] is a software tool that automatically extracts events from text such as news reports. In Sect. 4 we will use KEDS data for the Balkans region. Formally, an event series is a sequence  $a_1, \dots, a_k$  of tuples  $a_i = (t_i, s_i, o_i, c_i)$ , where

- $t_i$  is the *time-stamp* (date, given by the day),
- $s_i$  is the *subject* (source actor),
- $o_i$  is the *object* (target actor), and
- $c_i$  is the *code* (event type)

of event  $a_i$ . We say that actors  $s_i$  and  $o_i$  are *involved* in event  $a_i$ . Events are classified using the World Event/Interaction Survey (WEIS) codes [25]. Each event is assigned Goldstein weights  $-10 \leq \omega(a_i) = \omega(c_i) \leq 8.3$ , which are psychometrically determined scores depending only on the type of event (see [26]). A positive weight indicates the degree of *cooperation* of the corresponding type of event, whereas a negative weight measures *hostility*. Examples for Goldstein weights associated with event types are the following.

072	EXTEND MIL AID	8.3
054	ASSURE	2.8
160	WARN	-3.0
173	SPECIF THREAT	-7.0
223	MIL ENGAGEMENT	-10.0

Apparently, extending military aid is a highly cooperative action, whereas warnings are mildly hostiles and military engagement is extremely hostile. To analyze conflict, we will only make use of negatively weighted events, i. e. hostile actions.

The following excerpt indicates the coding of actors in the Balkans data.

```
NATO_OFFICIAL [NAT]
NATO-LED_STABILIZATION_FORCE_IN_BOSNIA [NAT]
SERBS_IN_BOSNIA [BOSSER]
RATKO_MLADIC [BOSSER]
MILOSEVIC [SERGOV 890101-971230] [FRYGOV 971231-001005] [SERSM >001006]
```

Several tokens in the news may be interpreted as referring to the same aggregated actor. In the above excerpt, NATO (NAT) is represented by (among others) potentially unnamed officials and SFOR.<sup>1</sup> Similarly, the actor BOSSER is represented by (among others) the general term “Serbs in Bosnia,” as well by specific persons like Ratko Mladić. On the other hand, the same token may represent different actors at different times. For

---

<sup>1</sup>The (Stabilisation Force) was a NATO-led multinational force in Bosnia and Herzegovina.

instance, Slobodan Milošević represents the Serbian government (SERGOV) until December 1997, the government of the Federal Republic of Yugoslavia (FRYGOV) until October 2000, and after being replaced by opposition-list leader Vojislav Koštunica only himself (SERSM).

Given an actor coding, textual statements are parsed into events like the following example which took place on 10 July 1995.

```
950710 NAT BOSSER 173 (SPECIF THREAT) POSSIBLE AIR STRIKES
```

This event is an action initiated by the NATO (active) and directed at the Serbs in Bosnia (passive). In addition to the event code (173), a textual description of the type of event (in this case a “specified threat”) is given in parentheses. The rest of the line is the stemmed form of the text fragment that has been turned by the KEDS parser to the corresponding event. Often, this text gives valuable additional information, in this case information about the nature of NATO’s threat. Datasets derived from serious conflicts can be quite large. For instance, the KEDS dataset encoding the Balkans conflict consists of more than 78,000 events.

To detect emergent patterns and utilize indirect relations, we transform the data into a network. Any set  $\{a_1, \dots, a_k\}$  of events gives rise to a directed and weighted interaction graph  $G = (V, E, \omega)$  that we call a *conflict network*. This graph  $G$  is made of a set  $V$  of vertices, a set  $E$  of edges and a set  $\omega$  of weights, in the following way. The network’s actor set  $V$  is the set of actors involved in any event as the source or the target, i.e.,  $V = \bigcup_{i=1}^k \{s_i, o_i\}$ . There is a directed edge  $e = (u, v) \in E$  if there is an event with source  $u$  and target  $v$ , and we assign a weight  $\omega(e)$  that is minus the sum of all negative weights on events initiated by  $u$  and directed to  $v$  (i.e., edge weights are positive and indicate the degree of hostility; cooperative events are disregarded).

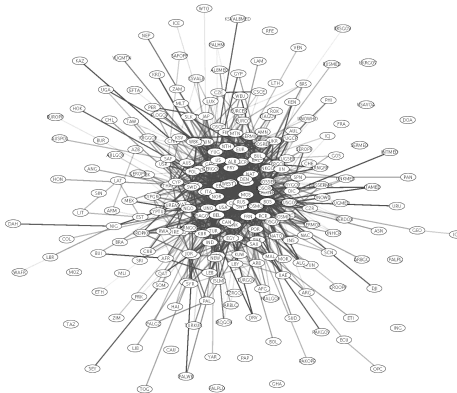


**Figure 2.** Force-directed drawing of hostile interaction in the Balkans from 1991 until 1997. The darkness of the edges is proportional to cumulative hostility weights. This kind of graph visualization is inappropriate for conflict networks as it does not distinguish between important and non-important actors nor does it reveal the structure of the network. In this chapter we present a method to draw conflict networks in a concise and easily understandable way (see Fig. 1).

Figure 2 shows an example of a conflict graph drawn by standard force-directed layout techniques [27]. The complexity of Fig. 2 already indicates the insufficiency of

general-purpose graph drawing techniques and the need for other analysis and visualization methods that are more appropriate for this application. In Sect. 2 we develop a method that extracts the dominant conflict structure, filters out minor actors, and produces a less complex image that is easy to understand.

It is unlikely that a focused data set yields an interaction graph with more than one significant non-trivial connected component. However, since connected components can be analyzed separately, we may safely assume that all interaction graphs are anyway connected.

## 2. Visualizing Conflict Structures

In this section we focus on extracting the structure of conflicts from static event data, i. e., we ignore time-stamps and consider the data to be given as a set rather than a sequence. The actors' positions are determined in a way where actors that are strongly in conflict with each other are far apart in the drawing and actors that are not connected by a conflictive edge, but have conflicts with the same other actors, are drawn closely together. Thus, the drawings facilitate the recognition of groups of actors that fight the same enemy. We start in Sect. 2.1 with the assumption that the network contains only one major bipolar conflict. This rather restrictive assumption is generalized in Sect. 2.2 to multipolar conflicts and in Sect. 2.3 to several parallel conflicts that overlap in the data set. The static methods that are developed in this section will be augmented to include dynamics in Sect. 3.

During the computation of the conflict network's group structure we will ignore edge directions. The rationale behind this is that if there is a strong negative (i. e., hostile) edge between actors  $u$  and  $v$ , then  $u$  and  $v$  should be in different groups—*independent* of whether the edge is directed from  $u$  to  $v$  or vice versa. However, edge directions will be taken into account when determining whether an actor is more active or more passive and highly asymmetric edges will also be shown as such.

### 2.1. Single Bipolar Conflict

A first attempt to determine the two opponent groups of a bilateral conflict would be to try to divide the actor set  $V$  into two disjoint subsets  $U$  and  $W$ , such that all edges go from  $U$  to  $W$  or vice versa and, hence, no edge connects two actors of the same group. See Fig. 3 for a fictitious conflict network of selected Balkan actors (the real network of these actors is much more complex) and the matrix  $P$  of derived group-membership values.

However, the discrete assignment of actors to the two groups of a bipartite conflict is completely impractical for empirical data. Firstly, the requirement that all conflictive relationships must be between the groups, and hence none of them within any group, is typically not supported by the data. Secondly, the attempt to determine a partition of  $V^2$  such that the sum of edge weights between the two groups is maximized is impractical as well: the problem is computationally intractable, highly sensitive to noise, requires actors to be purely in one group or the other, and reveals no prominence of actors.

---

<sup>2</sup>The groups  $U$  and  $W$  form a partition of  $V$  if their union equals  $V$  ( $V = U \cup W$ ) and their intersection is empty ( $U \cap W = \emptyset$ ).

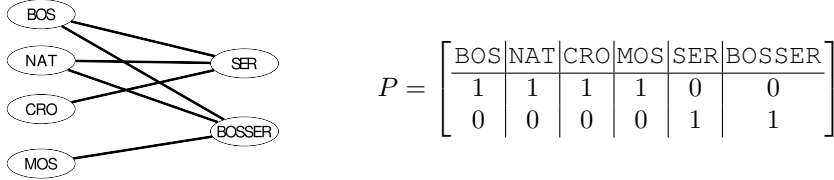


**Figure 3.** Visualization of a fictitious network that constitutes a bipartite conflict structure. The group-membership values are shown in matrix  $P$ . Actors are either entirely (value of one) or not at all (value of zero) in a given group.

We relax the idea of a strict bipartition by employing the recently introduced framework of structural projections and the closely related structural similarities [28]. This will lead us to a method that poses no algorithmic problems, is robust to noise, can handle actors that are members of both groups, and filters out unimportant actors on the fly. Instead of mapping actors to one class or the other, structural projections yield real-valued degrees of membership to classes. For a relaxed bipartition, actors that are strong members of one group have major conflicts with actors that are strong members of the other group but only minor conflicts with actors in their own group.

An example of visualization of such a real-valued assignment is shown in Fig. 4; the associated group-membership values of the most involved actors are in matrix  $P$  (1).

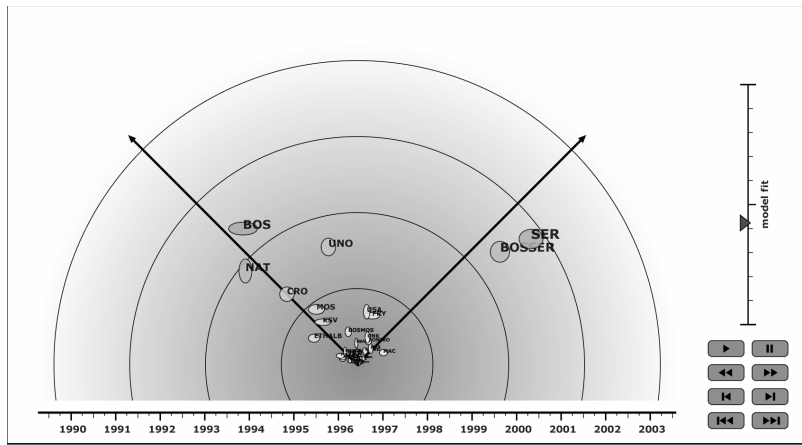


**Figure 4.** Bipolar visualization of Balkan conflict 1989–2003. Dominant actors include those set out in Fig. 3. Actors are members of the first or second group to the extent that they are mapped close to the left or right coordinate axis, respectively. (See the membership values of the most important actors in matrix  $P$  (1).) The angle (left vs. right) encodes the ratio between the two group's membership values. Involvement of actors is proportional to the distance from the origin. The aspect ratio (shape) of an actor encodes the ratio between activeness (height) and passiveness (width).

$$P = \begin{bmatrix} & \text{BOS} & \text{NAT} & \text{CRO} & \text{MOS} & \text{UNO} & \text{SER} & \text{BOSSER} & \dots \\ \text{BOS} & .7 & .5 & .3 & .2 & .5 & 0 & 0 & \dots \\ \text{NAT} & 0 & 0 & 0 & 0 & .2 & .8 & .7 & \dots \end{bmatrix} \quad (1)$$

Note that the degree of membership assigned to actors varies. E.g., **BOS** is a much stronger member of the first group (value of 0.7) than, e.g., **CRO** (value of 0.3). On the other hand **UNO**, though closer to the first group (degree of membership is 0.5), is also a member of the second group (degree of membership is 0.2), because conflicts with other actors in the first group (e.g., with **Bosnia**) are reported. Many of the unimportant actors close to the origin are filtered out because their level of hostility is not sufficient to place them prominently in one group or the other. Thus, our method not only determines a relaxed bipartition, but also indicates which actors are most responsible for the division.

The determination of the optimal membership values so that the weight of edges between the groups is maximized is derived in [24]. (Also see [28] for the general framework of this method.) Here we reproduce the results only.

*Group-membership values.* Given a conflict network  $G = (V, E, \omega)$  on  $n = |V|$  actors, let  $A$  be the symmetric adjacency matrix of  $G$ , defined as the  $n \times n$  matrix whose rows and columns are indexed by the actors of  $G$  and where the entries are defined by  $A_{uv} = A_{vu} = \omega(u, v) + \omega(v, u)$ .

1. Compute maximum and minimum eigenvalues  $\lambda_{\max}$  and  $\lambda_{\min}$  of  $A$  together with associated normalized eigenvectors  $v_{\max}$  and  $v_{\min}$ .
2. Let  $P$  be the  $2 \times n$  matrix with  $x = (v_{\max} + v_{\min})/\sqrt{2}$  in the first and  $y = (v_{\max} - v_{\min})/\sqrt{2}$  in the second row.
3. The membership values of actor  $v$  are the two real values in the column of  $P$  that is associated to  $v$  (see (1) for an example).
4. The *involvement* of actor  $v$  is defined to be the norm of its membership values, i.e., the involvement is  $\sqrt{P_{1v}^2 + P_{2v}^2}$ .

Any eigenvector algorithm for real symmetric matrices can be used in Step 1 (see, e.g., [29]), and there are many readily available software packages.

*Activeness or passiveness of actors.* *Activeness* is defined as the net weight of the events in which an actor is involved as the subject initiating the event, i.e., activeness of actor  $v$  is the value  $\sum_{u \in V} \omega(v, u)$ . Symmetrically, *passiveness* adds weights of events received, i.e., passiveness of actor  $v$  is the value  $\sum_{u \in V} \omega(u, v)$ .

*Indicator for the fit of the bipolar conflict model.* The *bipolarity* (or fit to the bipolar model) is defined as the ratio between the minimal and maximal eigenvalue, i.e.,

$$\beta(G) = \left| \frac{\lambda_{\min}}{\lambda_{\max}} \right| .$$

The index  $\beta(G)$  measures to what extent are conflicts only between the two groups and ranges between zero and one. It is one if and only if the graph is bipartite (i.e. if the model fits perfectly) and it is zero if and only if there are as many conflicts within the groups as there are in-between (i.e., if the model does not fit at all).

### 2.1.1. Graphing Bipolar Conflict Space

The graphical attributes of our visualization are determined as follows. The actors' position in the two-dimensional drawing indicate their group membership and involvement: Actors are mapped in direction of the left or right coordinate axis to the extent that they are members of the first or second group, respectively. We propose a coordinate system

where the x-axis points to the upper left corner and the y-axis to the upper right corner. This coordinate system seems to be preferable to the more usual one (one axis vertical, one horizontal) since it prevents the misguided interpretation of superiority of one group over the other. The angle (left vs. right) encodes the ratio between the two group membership values. The ratio between activeness and passiveness determines the aspect ratio (height vs. width) of a node, so that actors who initiate conflictive interactions, but are not the subject of retaliation are high and narrow. Involvement is proportional to the distance from the origin and emphasized in the size of an actor. Finally, we indicate the fit of the bipolar model using a bipolarity gauge on the right-hand side of the images.

Figure 4 shows the bipolar visualization of the network derived from the Balkan Conflict from 1989 to 2003. The circles around the origin link points of identical involvement. They help see that the most involved actor during the whole period of time is Serbia (SER), closely followed by the Serbs in Bosnia (BOSSER) and Bosnia (BOS). The bipolarity of this network is rather low (only around 0.42), indicating many conflicts within groups. Despite the low level of model fit, our method still yields two reasonable opponent groups: Serbia and the Serbs in Bosnia opposed to Bosnia and Croatia (CRO). The NATO (NAT) is opposed to SER and BOSSER, due to the massive air strikes in 1994 and 1995. Since NATO initiated more events than it receives (i.e., is more active than passive), it is displayed as a high and narrow actor.

## 2.2. Multipolar Conflict

The low fit of the bipolar conflict model to the complete Balkan data set (Fig. 4) indicates that many conflicts occur within groups and hence the assumption of only two opposing groups is not satisfactory. We call a conflict structure where  $k \geq 2$  groups are mutually in conflict a *k-lateral* conflict (for  $k = 2$  we get a bilateral conflict). Here we extend the method developed so far to deal with *k*-lateral conflicts. Doing this is straightforward from the analysis point of view, although the visualization has limitations if *k* gets larger than three for two-dimensional visualizations. The reason for these limitations is that it is not possible to draw four or more points in a two-dimensional space such that all pairs are at the same distance. In the following we derive a method to draw conflict networks in a two-dimensional image that reveals more general than just bilateral conflict structures.

The position of a particular actor in the drawing should express which other actors it confronts. If two actors  $u$  and  $v$  are connected by a hostile edge of large weight, then we want to draw  $u$  and  $v$  on opposite sides of the image. The difficulty lies in the fact that we have to draw not only two authors but the whole network such that all confronting pairs are simultaneously as far from each other as possible. This objective, which contrasts to most objective functions for graph drawing that traditionally want to keep edge lengths short [27], is of course due to the fact that edges encode negative relations. The good news is that this problem is efficiently solvable, as will be derived next.

Let  $G = (V, E, \omega)$  be the conflict network with actor set  $V$  of cardinality  $n = |V|$  and let  $A$  be its symmetric adjacency matrix (as defined in Sect. 2.1). Since we want to draw the conflict network in two-dimensional space, the positions of all  $n$  actors are represented by two vectors  $x, y \in \mathbb{R}^n$ . If for two actors  $u$  and  $v$  the entry  $a_{uv}$  in the adjacency matrix is large (i.e., if they are strongly in conflict), then they are well-represented by the coordinate vector  $x$  if the entry  $x_u$  is (say) strongly negative and the entry  $x_v$  strongly positive. Then, the value  $x_u a_{uv} x_v$  is negative and has a quite large

absolute value. Summing this up over all pairs of actors,  $x$  is determined to minimize the objective function

$$\Phi_A(x) = \sum_{u,v \in V} x_u a_{uv} x_v = x^T A x ,$$

under the condition that  $x$  must have unit length to keep the drawing to the screen size. It follows from an alternative description of the eigenvalues of a matrix that this term is minimized if and only if  $x$  is equal to the eigenvector of  $A$  associated to the smallest eigenvalue  $\lambda_{\min}$  (see, e.g., [29]). The second coordinate vector  $y$  is chosen to minimize  $\Phi_A(y)$  under the condition that  $y$  is normalized and orthogonal to  $x$ . This is solved by taking for  $y$  the eigenvector of  $A$  associated to the second smallest eigenvalue  $\lambda'_{\min}$ .

This method can reveal network structures beyond bilateral conflicts. For instance, Fig. 5 shows the visualization of the Balkan Conflict network (1989–2003). Three groups can be detected whose dominant members are  $\{\text{BOS}\}$  (first group),  $\{\text{BOSSER, SER}\}$  (second group), and  $\{\text{UNO, NAT}\}$  (third group). However, actors are not strictly assigned to one or the other group but their membership can also be intermediate. For instance, conflicts that are reported between UNO and BOSSER (Serbs in Bosnia) are stronger than conflicts between UNO and SER, which leads to the drawing in Fig. 5 where BOSSER is more distant to UNO than SER to UNO. Actor CRO (Croatia) is much less involved and therefore drawn smaller and closer to the origin in the center of the drawing than the aforementioned five actors. CRO has strong conflicts with the second group (most notably with SER) but no strong conflicts are reported between CRO and either members of the first or third group. Therefore, CRO is drawn exactly opposite to SER and between the first and third group.

Note that the complete Balkan data set indeed yields three groups that are mutually in conflict. In particular, it is not possible to assign the Balkan actors to only two groups without having strong conflicts within a group, leading to the low fit of the bipolar model (Fig. 4).

The visualization of the Gulf Conflict network (1979–1999) (see Fig. 6) does *not* reveal three groups. Instead we can see a bilateral conflict ( $\text{ISR}$  vs.  $\text{LEB}$ ) overlaying a trilateral conflict that is mostly formed by  $\text{USA}$ ,  $\text{IRQ}$ , and  $\text{IRN}$ . In Sect. 2.3 we extend our method to handle such situations.

*Interpolation between bipolar and tripolar conflicts.* One further detail has to be taken care of: a conflict is not necessarily either bilateral or trilateral but can show an intermediate structure. For instance, Fig. 7 shows the conflict structure among a selected subset of Gulf actors involved in conflicts in Iran and Iraq. The dominant structure is a triangle formed by  $\text{USA}$ ,  $\text{IRQ}$ , and  $\text{IRN}$ . However, conflicts reported between  $\text{USA}$  and  $\text{IRN}$  are weaker than those reported between  $\text{IRQ}$  on one side and  $\text{USA}$  or  $\text{IRN}$  on the other side. The question arises whether this network is best represented by a balanced tripolar structure similar to Fig. 5 (which would ignore that two of the three actors are closer to each other than to the third), or by a bipolar structure placing  $\text{IRQ}$  on one side and  $\text{USA}$  along with  $\text{IRN}$  on the other (which would ignore the hostile edge between  $\text{USA}$  and  $\text{IRN}$ ). We argue that the best way to represent such a conflict structure lies in the middle, i.e., to show it as an intermediate between a bipolar and a balanced tri-polar conflict. Figure 7 shows a triangle which has three unequal sides, but where  $\text{USA}$  and  $\text{IRN}$  are closer to each other than to  $\text{IRQ}$ . Such a representation can be computed by appropriately scaling

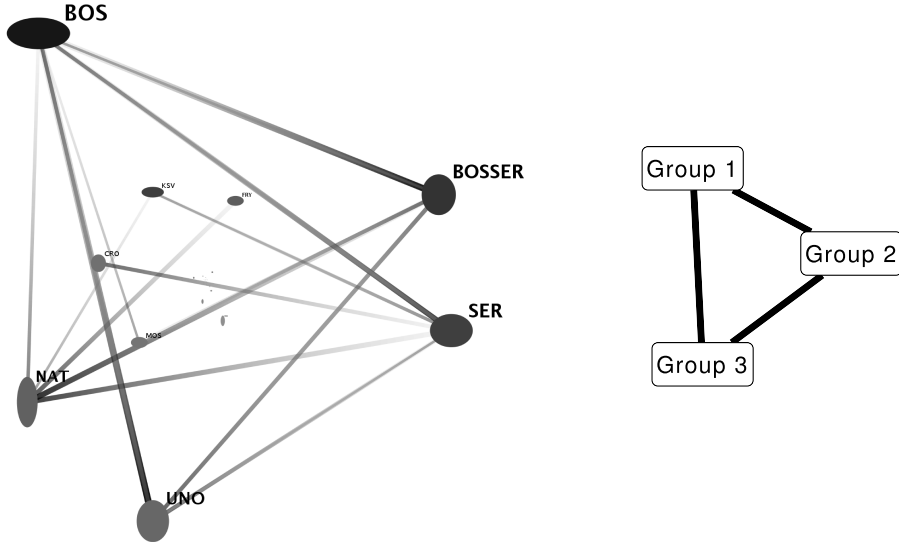


**Figure 5.** The graph on the left-hand side visualizes the conflict network arising from the Balkan Conflict 1989–2003. This network matches well the model of a trilateral conflict shown on the righthand side. Three groups that are mutual in conflict are revealed whose dominant members are {BOSSER, SER}, {UNO, NAT}, and {BOS}. The black-white gradient of the edges indicates the main direction. For instance, the edge from NAT directed to SER has a higher weight than the reverse edge from SER to NAT, meaning that more actions were directed from NATO to the Serbs than the reverse.

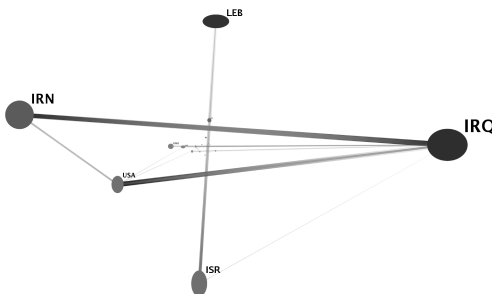


**Figure 6.** Visualization of Gulf Conflict 1979–1999: Two overlapping dominant conflicts can be detected. The trilateral conflict model shown in Fig. 5 (right) does not fit well to this network. A remedy for this fact is to separate almost independent conflicts first, as will be described in Sect. 2.3.

the eigenvectors we project on (see the algorithm description in Sect. 2.4). If the weight of the edge between USA and IRN got smaller and smaller, then these two actors would move towards each other until the pattern of a purely bipolar conflict is reached.

### 2.3. Parallel Conflicts

The complete data set for the Gulf Conflict (1979–1999) did not match well a bilateral nor a trilateral conflict model (see Fig. 6), since it consists of two almost independent conflicts: that between ISR and LEB on one hand and the mutual conflicts between USA,

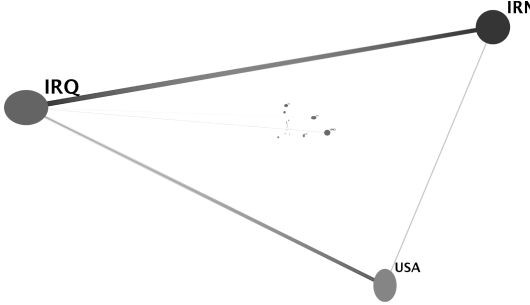


**Figure 7.** The dominant cluster in the Gulf Conflict data set (1979–1999) contains USA, IRQ, and IRN and shows a tri-polar structure, although a higher conflict intensity is reported between the pairs (IRQ,IRN) and (IRQ,USA) than between (USA,IRN).

IRQ, and IRN on the other. A way to obtain a better visual representation of this data set is to first separate almost independent conflicts into different sub-networks and then visualize these independently as described before. The separation of independent conflicts can be done either by a network clustering algorithm that computes dense clusters (corresponding to subsets of actors that are strongly in conflict) or interactively by the analyst who chooses a subset of actors he or she is interested in.

The Gulf Conflict data set contains three significant clusters that have been obtained by a slight adaptation of a spectral clustering technique [30]. The strongest one (already shown in Fig. 7) has a mostly tri-polar structure. The two other conflict clusters (that have a very trivial bipolar structure) can be seen in Fig. 8. The formerly overlaying conflicts (see Fig. 6) are now displayed separately, each according to its structure.



**Figure 8.** The remaining two of the three major clusters in the Gulf Conflict data set (1979–1999) (the cluster containing USA, IRQ, and IRN has been shown already in Fig. 7) have a trivial bipolar structure and are shown in the above two diagrams.

#### 2.4. Visualization Algorithm

We summarize the method outlined in this section in the following algorithm for the two-dimensional visualization of conflict networks. The algorithm takes as input a directed graph  $G = (V, E, \omega)$  where the weight  $\omega(u, v)$  of an edge  $(u, v)$  is determined by the conflictive actions targeted from actor  $u$  to actor  $v$ .

1. Divide the actor set into dense clusters  $C_1, \dots, C_p$ , either by a clustering algorithm (such as [30]), or manually during data analysis.
2. For all clusters  $C$ , compute  $A$  as the symmetric adjacency matrix of the subgraph defined by  $C$  and perform the following steps to visualize  $C$  (let  $n = |C|$  denote the number of actors in  $C$ ).
  - (a) Compute the two minimal (negative) eigenvalues  $\lambda_{\min}$  and  $\lambda'_{\min}$  of  $A$  together with (orthogonal and normalized) eigenvectors  $x$  and  $y$ .

- (b) Construct the  $2 \times n$  matrix  $P$  whose first row is equal to  $x$  and whose second row is equal to  $y \cdot \frac{\lambda'_{\min}}{\lambda_{\min}}$  (i.e.,  $y$  scaled with the ratio of the next-to-minimal eigenvalue divided by the minimal eigenvalue).
- (c) Draw actor  $v$  as an ellipse at the position defined by the  $v$ 'th column of  $P$ . The ratio height/width of the ellipse is proportional to the outdegree/indegree (i.e., activeness/passiveness) of  $v$ . The product of height with width (proportional to the area of the ellipse) is proportional to the Euclidean length of the  $v$ 'th column of  $P$  (encoding  $v$ 's involvement).
- (d) Draw the strongest edges of the subgraph defined by  $C$  (the number of edges drawn is a free parameter). The width of an edge  $(u, v)$  is proportional to the symmetric weight  $\omega(u, v) + \omega(v, u)$ . A dark-grey to light-grey color gradient is directed from  $u$  to  $v$  if  $\omega(u, v) > \omega(v, u)$  and directed from  $v$  to  $u$  if  $\omega(u, v) < \omega(v, u)$ . The darker side of this gradient is a fixed grey-value (close to black). The lighter side is this grey value scaled with  $\omega(v, u)/\omega(u, v)$  if  $\omega(u, v) > \omega(v, u)$ , so that the gradient becomes more pronounced if the ratio gets larger.

An example of a strongly skewed edge is that from NAT directed to SER in Fig. 5. Note that the side closer to NAT is darker than the side closer to SER.

### 3. Animating Conflict Dynamics

The images generated as described in Sect. 2 already reveal the actors and conflicts that are dominant over the whole period of time. However, due to varying conflict intensity and changing oppositions and alliances these images might not represent well the structure at specific time-points. Likewise, conflicts of short duration might be filtered out. To obtain a more detailed insight into the evolution of conflicts, we will introduce a technique for smooth animation of the above type of scatterplots for limited periods of time.

The event graph  $G$  is used to generate a sequence of graphs  $G_t$ , each of which represents the view on the set of events at the specific time  $t$ . A graph  $G_t$  yields one frame of the final video and this frame shows a detailed image of the situation at time  $t$ . How the events are viewed at a certain time-point is determined by a *scaling function*  $\eta: \mathbb{R} \rightarrow \mathbb{R}_{\geq 0}$ , which models how events move into the data when time increases and how they fade out. Examples of possible scaling functions are triangular shaped scaling functions with time radius  $r$ , as defined and illustrated in Fig. 9. The function  $\eta_r$  does not

$$\eta_r(t) = \begin{cases} (t+r)/r & \text{if } |t| \leq r \text{ and } t < 0 \\ -(t-r)/r & \text{if } |t| \leq r \text{ and } t \geq 0 \\ 0 & \text{if } |t| > r \end{cases} .$$

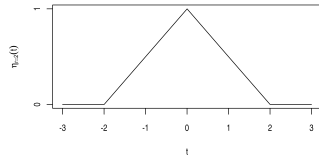


**Figure 9.** *Left:* Definition of the triangular shaped scaling function  $\eta_r$  with time radius  $r$ . *Right:* Illustration of  $\eta_r$  for  $r = 2$ .

consider events with a time-stamp more than  $r$  away from the current time-point. Events

move into  $G_t$  linearly until  $t$  is larger than their time-stamp. Then, they fade out linearly until they have zero weight.

For a fixed scaling function  $\eta$  and time point  $t$ , the graph  $G_t = (V, E, \omega_t)$  is defined as follows. The actor set  $V$  and the edge or event set  $E$  are the same as for the input graph  $G$ . The weight  $\omega_t(e)$  of an event  $e$  at time  $t$  is defined to be  $\omega_t(e) = \omega(e) \cdot \eta(t_e - t)$ , that is, the weight of  $e$  at time  $t$  is its absolute weight  $\omega(e)$  times a scaling factor which is dependent on the difference between the time-stamp  $t_e$  of the event and the current time  $t$ . The graph  $G_t$  may be reduced by removing events with zero weight, as well as isolated actors, since these do not influence the analysis and would be invisible in the final video.

Given a graph  $G$ , representing a list of events, the movie is generated by the following steps.

1. Select a sequence of time-points  $t_1 < \dots < t_N$  in a given time interval.
2. For each  $i$  from 1 to  $N$ 
  - Compute the visualization of the graph  $G_{t_i}$ .
3. The images for all time-points yield the frames of the video.

In order to maintain the overall appearance of the frames one further detail has to be taken into consideration. If  $v$  is an eigenvector of  $A$  associated to eigenvalue  $\lambda$ , then so is  $-v$ . Thus the eigensolver algorithm could return either  $v$  or  $-v$  as a solution to the eigenvalue problem. To prevent that this assignment switches from one frame to another (which would result in interchanging the axes of the coordinate system from one frame to another) we have to ensure that the eigenvectors we use point in a well-defined direction.

For the bipolar conflict projection the canonical direction for the eigenvector  $v_{\max}$  associated to the largest eigenvalue is simply the direction in which each entry of  $v_{\max}$  is positive. (It is standard knowledge in algebraic graph theory that all entries of this eigenvector have the same sign.) We define the canonical direction for the eigenvector  $v_{\min}$  for time-step  $t$  recursively by the direction of this eigenvector for time-step  $t - 1$ . The direction of  $v_{\min}$  is chosen such that the angle between  $v_{\min}$  at time  $t$  and  $v_{\min}$  at time  $t - 1$  is smaller than 90 degrees. Thus, only the direction of  $v_{\min}$  for the very first time-step is arbitrary. This translates to the fact that there is no absolute meaning attached to the two opponent groups. A second computation of the movie could interchange the first and second group, but then it has to reverse the assignment for all actors and at all time points, which results in the same opponents.

For multipolar conflicts the computed coordinates are only unique up to rotation or reflexion of the two-dimensional image space. To ensure that the images are not rotated or reflected from one image to the next we determine the two-dimensional orthogonal transformation that minimizes the distance between images at time  $t$  and time  $t - 1$  and apply it to the drawing at time  $t$ . More precisely, let  $t$  be a time-point that is not the first and let  $P_{t-1}$  be the  $2 \times n$  matrix holding the two-dimensional coordinates of all  $n$  actors at time  $t - 1$ . Further, let  $P_t$  be the  $2 \times n$  matrix as returned by the eigensolver at time  $t$ . Set  $X = P_{t-1}P_t^T$  and compute the *Singular Value Decomposition* (SVD)  $X = USV^T$  of  $X$  [29]. The optimal coordinates at time  $t$  are given in the matrix  $P'_t = UV^T P_t$ .

Of course, animation can also be applied to sub-networks representing independent conflict clusters.

In Fig. 10 we show three selected time points in the Gulf Conflict cluster containing USA, IRQ, and IRN. In the smooth animation, the radical change of the relative positions of USA and IRQ can be easily followed.

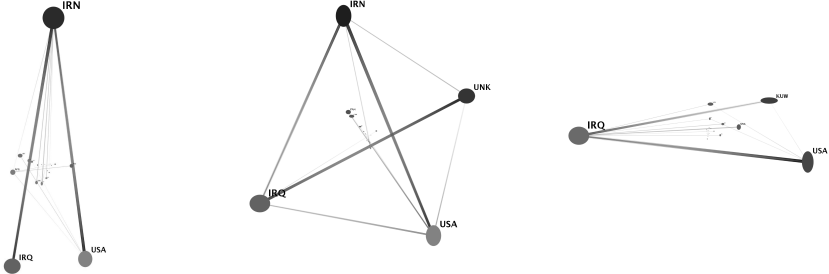


**Figure 10.** Dynamic visualization of Gulf Conflict (cluster containing USA, IRQ, and IRN) (*left*: June 1989, *middle*: March 1990, *right*: August 1990). Note that especially the relative positions of USA and IRQ changed completely during this period.

#### 4. Application Example

We apply our method to visualize a data set from the Kansas Event Data System (KEDS) [5] (see Balkan data set [5]) in a prototypical implementation. The animations<sup>3</sup> are realized in SVG format (Scalable Vector Graphics, see W3C Recommendation at <http://www.w3.org/TR/SVG/>), thus they can be viewed on any web browser with an appropriate plug-in.

##### 4.1. Dynamic Bipolar Visualization

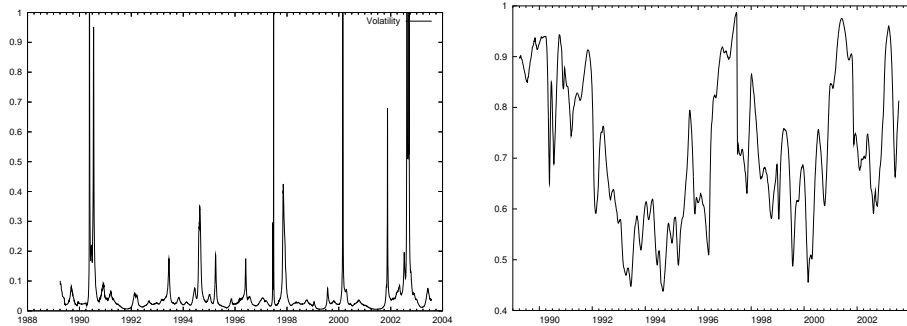


**Figure 11.** *Left*: Volatility profile of the bipolar visualization of the Balkan conflict. *Right*: Bipolarity (fit of the bipolar model) of the Balkan Conflict.

The varying degree of polarization can be inferred from the model fit indicator curve in Fig. 11 (*right*). Although there is great variation in the magnitude of the model fit, it is often close to one and at all time points considerably distant from zero. Thus, the simplistic assumption of bipartite conflicts already fits the data sufficiently well—if we restrict the analysis to relatively short time intervals. (As it has been noted before, summarizing the whole data set over 14 years in a bipolar model provides suboptimal results, e.g. see Figs. 4 and 5.) The *volatility* indicator [24] measures the sensitivity to noise of

<sup>3</sup>The animation of the bipolar visualization are available from <http://www.inf.uni-konstanz.de/algo/research/conflict/>

our drawing technique. The volatility profile for the Balkan conflict is shown in Fig. 11 (*left*). The fact that this indicator is small during most time-steps gives guarantees the stability of our method. The peaks in this plot, where the volatility reaches a value of one, can be recognized in the animation by a sudden movement of the actors.

The following figures show selected time-points of the Balkans conflict.

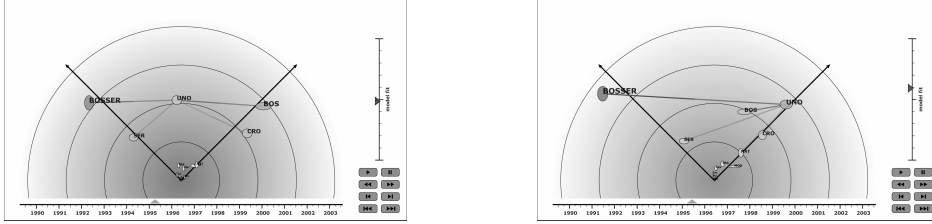


**Figure 12.** War in Bosnia, first semester 1995 (only edges incident to UNO are shown). *Left*: Two opposing groups and UNO trying to mediate. *Right*: BOSSER's troops in conflict with the UN. The heavy edge pushes UNO to the group on the right-hand side.

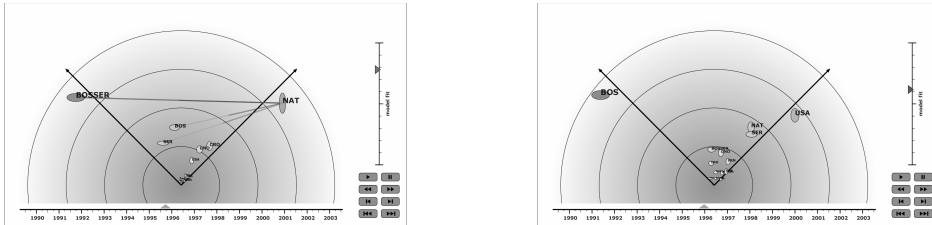


**Figure 13.** *Left*: NATO bombing in Bosnia, second semester 1995. Note that BOSSER changed from high and narrow (being the source of events) in Fig. 12 (*right*) to broad and flat (being a target). *Right*: Dayton peace talks.

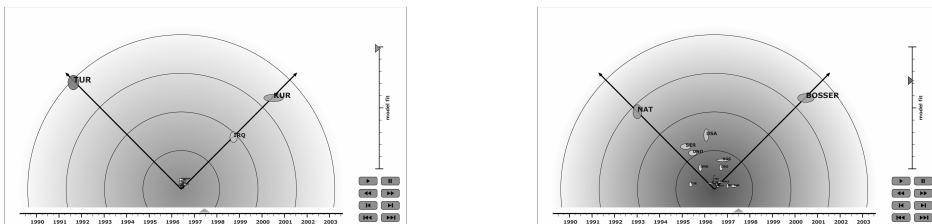


**Figure 14.** *Left*: Conflict between Turkey and the Kurds before the change from Reuters North America to Reuters Business Briefing (June 1997). *Right*: During the change: TUR and KUR are still visible to the left and to the right of the origin and are rapidly moving towards it.

Important changes in the conflict structure took place in 1995 and 1996. Figure 12 (*left*) shows the war in Bosnia, where Serbia and the Serbs in Bosnia (BOSSER) are opposed to Bosniaks and Croats. The UNO, which is trying to install peace in Bosnia, has conflicts of similar strength to all of them. This changes when troops of the Bosnian Serbs captured weapons from UN peace keepers and declined to return them (Fig. 12*right*). After the Bosnian Serbs did not respond to an ultimatum, the NATO started air strikes

under the order of the UN (Fig. 13*left*). The opposing parties finally participated in peace talks which took place in Dayton, Ohio and were signed in December 1995 (Dayton Peace Agreement, Fig. 13*right*). After this, events in the Balkans calmed down and the media focused on the conflict between Turkey and the Kurds.

The conflict between Turkey and the Kurds also exemplifies a problem with the data that we were not aware of before seeing the animation. In July 1997, there is an abrupt change in media coverage in the sense that reports on hostilities between Turks and Kurds are suddenly missing. Figure 14 shows the conflict structure in the Balkans with only a few days in between. The change is also visible in a significant drop in the bipolarity curve (Fig. 11*right*), where the highly bipolar situation rapidly changes into a more complex one, and in a peak in the volatility curve (Fig. 11*left*).

That this change is indeed supported by the data can be verified by printing the events involving TUR and KUR. During a period of one month from May 10<sup>th</sup> 1997 to June 10<sup>th</sup> 1997 many hostile events between these two actors are reported (see Fig. 15).

970514 TUR KUR (MIL ENGAGEMENT) KILLED
970514 TUR KUR (MIL ENGAGEMENT) TROOPS CLASHED
970514 TUR KUR (MIL ENGAGEMENT) TURKISH PUSHED AGAINST KURDISH
970520 TUR KUR (MILITARY DEMO) HUNTING DOWN
970521 TUR KUR (MILITARY DEMO) BUILDING UP FORCES
970522 KUR TUR (MIL ENGAGEMENT) ATTACKED KILLING
970522 TUR KUR (MIL ENGAGEMENT) TURKISH PUSHED AGAINST KURDISH
970522 KUR TUR (NONMIL DEMO) STAGED PROTEST
970522 KUR TUR (DENIGRATE) CONDEMNATION
970524 KUR TUR (MIL ENGAGEMENT) ATTACKS ARMY
970526 TUR KUR (MIL ENGAGEMENT) TROOPS CLASHED
970527 TUR KUR (MIL ENGAGEMENT) BOMBED
970602 TUR KUR (MIL ENGAGEMENT) KURDISH KILLED IN TURKISH
970604 TUR KUR (MIL ENGAGEMENT) KURDISH KILLED IN TURKEY
970604 TUR KUR (ARREST PERSON) JAIL
970605 TUR KUR (MIL ENGAGEMENT) KILLED
970607 TUR KUR (DENY) DENIED
970609 TUR KUR (DENY) DENIED
970610 KUR TUR (DEMAND) DEMANDING

**Figure 15.** Hostile events between TUR and KUR from 05/10/97 to 06/10/97.

In contrast, during a period of one month from 11 June 1997 until 11 July 1997 there is *no* hostile event reported between TUR and KUR. There are no prominent historic events explaining this sudden “peace”. However, turning to the data description gives the information that this is precisely the time when KEDS sources change from Reuters North America to Reuters Business Briefing, with the latter apparently not covering the conflict (or TUR and KUR being filtered out during preparation of the data for the KEDS parser).

#### 4.2. Multipolar Visualization of Independent Conflict-Clusters

The conflict network arising from the Balkan data set contains several interesting sub-networks corresponding to separate conflicts. Figure 16 shows six selected conflict clusters that have been identified by a spectral clustering technique [30]. Note that some of these sub-networks have a trilateral structure (such as the war in Bosnia shown at the top-left). Other clusters have a purely bipolar structure, as e. g., Slobodan Milošević (SERSM) versus the UN War Crime Tribunal (UNWCT) shown at the bottom-right. Yet other sub-conflicts have an intermediate structure, as e. g., conflicts on Cyprus shown at the top-right. Naturally, it could be argued that some of these conflicts should not be part of the Balkan data set. Thus, the visualization presented here may also serve as a support for data cleaning.

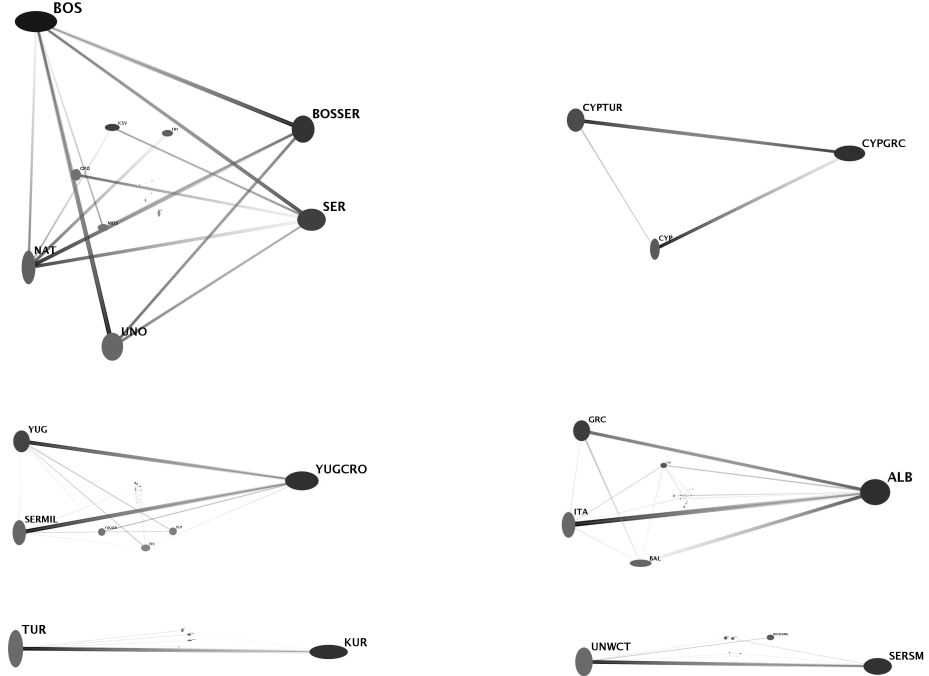


**Figure 16.** Strong conflict clusters in the Balkan data set.

While the six conflict sub-networks in Fig. 16 seem to be reasonable and correspond to known historic events, we detected another conflict cluster in the Balkan data set that surprised us. According to the network shown in Fig. 17, the USA-Government (USAGOV) would be a serious opponent of the USA.

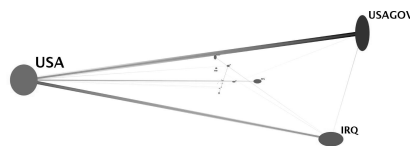


**Figure 17.** One conflict cluster found in the data set seems hard to believe. The hostile edge between USAGOV and USA is probably due to some systematic errors of the KEDS parser (see text for a more detailed description).

To find out the reason for this strange configuration we printed all major hostile events with weight  $< 5.0$  between these two actors in Fig. 18. Apparently the KEDS parser repeatedly interpreted certain recurrent statements in the news as military demonstrations of the US-Government targeted against the USA. (Military demonstration is a serious hostile event with weight =  $-7.6$ ; the most hostile event has weight  $-10.0$ .) Note that although, this error seems to be repeated quite often, the resulting conflictive edge would vanish against the hostilities between (say) BOSSER and BOS. In particular, it would not be visible without the prior clustering. The story around Fig. 17 is a good

930224 USAGOV USA (ARREST PERSON) ROUNDED UP
930714 USAGOV USA (MILITARY DEMO) SENDING TROOPS
930729 USAGOV USA (NONMIL THREAT) CONSIDERING STRIKES
940210 USA USAGOV (MIL ENGAGEMENT) FIRED AT PRESIDENT CLINTON'S
940525 USAGOV USA (MILITARY DEMO) SEND TROOPS
950104 USA USAGOV (CUT AID) EMBARGO
950803 USAGOV USA (CUT AID) EMBARGO
950929 USAGOV USA (MILITARY DEMO) SEND TROOPS
951008 USAGOV USA (MILITARY DEMO) SEND TROOPS
951119 USAGOV USA (MILITARY DEMO) SEND TROOPS
951119 USAGOV USA (MILITARY DEMO) SEND TROOPS
951120 USAGOV USA (MILITARY DEMO) SENDING TROOPS
951125 USAGOV USA (MILITARY DEMO) SEND TROOPS
951202 USAGOV USA (MILITARY DEMO) SEND TROOPS
951203 USAGOV USA (MILITARY DEMO) SEND TROOPS
951213 USAGOV USA (CUT AID) VOTED TO CUTTING OFF FUNDS
960113 USAGOV USA (MILITARY DEMO) INSPECTED TROOPS
960113 USAGOV USA (MILITARY DEMO) INSPECTED TROOPS
960203 USA USAGOV (ARREST PERSON) HOLDS
960711 USAGOV USA (MIL ENGAGEMENT) ASSAULT
960917 USAGOV USA (MILITARY DEMO) ORDERED TROOPS
961006 USAGOV USA (MILITARY DEMO) SENT TROOPS
970624 USAGOV USA (CUT AID) VOTED TO CUT OFF FUNDS
990501 USAGOV USA (SEIZE POSSESSION) EXPANDED
990504 USA USAGOV (MIL ENGAGEMENT) KILLED
010616 USA USAGOV (NONMIL DEMO) DEMONSTRATED

**Figure 18.** Hostile events between USA and USAGOV. Military demonstration is a serious event (weight= -7.6) that repeatedly has been interpreted by the KEDS parser as being targeted against the USA.

example to illustrate the utility of visualization for data cleaning and/or improvement of automatic event parsers.

## 5. Discussion

In this chapter we presented a general method for the visualization of conflict networks. We focused on the description of the visualization technique and briefly demonstrated its usefulness. The images produced give deep insight into the conflict structure and, as illustrated in the examples, may lead to the detection of coding errors.

A future ready-to-use conflict visualizer would certainly benefit from interaction possibilities allowing the analyst to trace back the events responsible for conflict edges and finally trace back the original news reports [24]. Another issue for future work is to augment the method to simultaneously visualize other relations (such as membership to official alliances, or geographic closeness) and supplementary attributes of the actors (such as ethnic composition, distinction between state and non-state actors etc.). Visualizing attribute data can be conveniently done by color or texture of the nodes representing actors.

## References

- [1] Kazuo Yamaguchi. *Event History Analysis*. Sage, 1991.
- [2] Nils Petter Gleditsch, Peter Wallensteen, Mikael Eriksson, Margareta Sollenberg, and Håvard Strand. Armed conflict 1946-2001: A new dataset. *Journal of Peace Research*, 39(5):615–637, 2002.
- [3] David Singer. The correlates of war project: Interim report and rationale. *World Politics*, 24(2):243–270, 1972.
- [4] Gary King and Will Lowe. An automated information extraction tool for international conflict data with performance as good as human coders: A rare event evaluation design. *International Organization*, 57:617–642, 2003.
- [5] Phillip A. Schrodt, Shannon G. Davis, and Judith L. Weddle. Political science: KEDS-a program for the machine coding of event data. *Social Science Computer Review*, 12(3):561–588, 1994. (Data sets available at <http://www.ku.edu/~keds/data.dir/balk.html>).

- [6] Gerald Schneider and Vera E. Troeger. War and the world economy: Stock market reactions to international conflicts, 1990–2000. *Journal of Conflict Resolution*, 50(5):623–645, 2006.
- [7] Massimo Guidolin and Eliana La Ferrara. The economic effects of violent conflict: Evidence from asset market reactions. Technical report, Federal Reserve Bank of St. Louis, 2005.
- [8] Gerald Schneider. Banking on the broker? Forecasting conflict in the levant with financial data. In Frank Wayman, Paul Williamson, and Bruce Bueno de Mesquita, editors, *Prediction: Breakthroughs in Science, Markets, and Politics*. University of Michigan Press, to appear.
- [9] Zeev Maoz, Ranan D. Kuperman, Lesley G. Terris, and Ilan Talmud. International relations: A network approach. In A. Mintz and B. Russett, editors, *New Directions for International Relations*. Lexington Books, 2004.
- [10] Zeev Maoz. Network polarization, network interdependence, and international conflict, 1816–2002. *Journal of Peace Research*, 43(4):391–411, 2006.
- [11] Zeev Maoz, Ranan D. Kuperman, Lesley G. Terris, and Ilan Talmud. Structural equivalence and international conflict. *Journal of Conflict Resolution*, 50(5):664–689, 2006.
- [12] Frank Harary. A structural analysis of the situation in the Middle East in 1956. *Journal of Conflict Resolution*, 5(2):167–178, 1961.
- [13] Zeev Maoz, Lesley G. Terris, Ranan D. Kuperman, and Ilan Talmud. What is the enemy of my enemy? Causes and consequences of imbalanced international relations, 1816–2001. *Journal of Politics*, 69(1):100–115, 2007.
- [14] Joan Esteban and Debraj Ray. A comparison of polarization measures. Technical report, UAB and CSIC, 2007. (available at <http://ideas.repec.org/p/aub/autbar/700.07.html>).
- [15] Joshua S. Goldstein, Jon C. Pevehouse, Deborah J. Gerner, and Shibley Telhami. Reciprocity, triangularity, and cooperation in the Middle East, 1979–97. *Journal of Conflict Resolution*, 45(5):594–620, 2001.
- [16] R. N. Rosecrance. Bipolarity, multipolarity, and the future. *Journal of Conflict Resolution*, 10(3):314–327, 1966.
- [17] August Hämerli, Regula Gattiker, and Reto Weyermann. Conflict and cooperation in an actors’ network of Chechnya based on event data. *Journal of Conflict Resolution*, 50(2):159–175, 2006.
- [18] James Allan, Rahul Gupta, and Vikas Khandelwal. Temporal summaries of news topics. In *Proc. ACM-SIGIR’01*, pages 10–18, 2001.
- [19] James Allan, Ron Papka, and Victor Lavrenko. On-line new event detection and tracking. In *Proc. ACM-SIGIR’98*, pages 37–45, 1998.
- [20] Clive Best, Erik Van der Groot, and Monica de Paola. Thematic indicators derived from world news reports. In *Proc. International Conference on Intelligence and Security Informatics (ISI 2005)*, pages 436–447, 2005.
- [21] Pak Chung Wong, Harlan Foote, Dan Adams, Wendy Cowley, and Jim Thomas. Dynamic visualization of transient data streams. In *Proc. IEEE Symp. Information Visualization (InfoVis ’03)*, pages 97–104, 2003.
- [22] John M. Chambers, William S. Cleveland, Beat Kleiner, and Paul A. Tukey. *Graphical Methods for Data Analysis*. Wadsworth, 1983.
- [23] William S. Cleveland and Robert McGill. The many faces of a scatterplot. *Journal of the American Statistical Association*, 79(388):807–822, 1984.
- [24] Ulrik Brandes, Daniel Fleischer, and Jürgen Lerner. Summarizing dynamic bipolar conflict structures. *IEEE Transactions on Visualization and Computer Graphics, special issue on Visual Analytics*, 12(6):1486–1499, 2006.
- [25] Charles A. McClelland. World event/interaction survey codebook (icpsr 5211), 1976.
- [26] Joshua S. Goldstein. A conflict-cooperation scale for WEIS international events data. *Journal of Conflict Resolution*, 36(2):369–385, 1992.
- [27] Michael Kaufmann and Dorothea Wagner, editors. *Drawing Graphs*. Springer Verlag, 2001.
- [28] Ulrik Brandes and Jürgen Lerner. Structural similarity in graphs. In *Proc. 15th Intl. Symp. Algorithms and Computation (ISAAC’04)*, pages 184–195, 2004.
- [29] Gene H. Golub and Charles F. van Loan. *Matrix Computations*. John Hopkins University Press, 1996.
- [30] Ravi Kannan, Santosh Vempala, and Adrian Vetta. On clusterings: Good, bad and spectral. *Journal of the ACM*, 51(3):497–515, 2004.